Spiking Neural Networks: A Stochastic Signal Processing Perspective

Hyeryung Jang, Osvaldo Simeone, Brian Gardner, and André Grüning

Abstract

Spiking Neural Networks (SNNs) are distributed systems whose computing elements, or neurons, are characterized by analog internal dynamics and by digital and sparse inter-neuron, or synaptic, communications. The sparsity of the synaptic spiking inputs and the corresponding event-driven nature of neural processing can be leveraged by hardware implementations to obtain significant energy reductions as compared to conventional Artificial Neural Networks (ANNs). SNNs can be used not only as co-processors to carry out given computing tasks, such as classification, but also as learning machines that adapt their internal parameters, e.g., their synaptic weights, on the basis of data and of a learning criterion. This paper provides an overview of models, learning rules, and applications of SNNs from the viewpoint of stochastic signal processing.

INTRODUCTION

Artificial Neural Networks (ANNs) have become the de-facto standard tool to carry out supervised, unsupervised, and reinforcement learning tasks. Their recent successes range from image classifiers that outperform human experts in medical diagnosis to machines that defeat professional players at complex games such as Go. These breakthroughs have built upon various algorithmic advances, but have also heavily relied on the unprecedented availability of computing power and memory in data centers and cloud computing platforms. The resulting considerable energy requirements run counter to the constraints imposed by implementations on low-power mobile or embedded devices for applications such as personal health monitoring or neural prosthetics.

ANN vs SNN. Various new hardware solutions have recently emerged that attempt to improve the energy efficiency of ANNs by exploring the trade-off between complexity and accuracy in the implementation of tensor operations. A different line of work seeks instead for an alternative framework that moves away from conventional ANNs by taking inspiration from the human brain. The human brain is capable of performing general and complex tasks at a minute fraction of the power required by state-of-the-art supercomputers. Insights from neuroscience suggest that sparse, event-driven, space-time computing as

enabled by networks of spiking neurons may be among the main reasons for the energy efficiency of the brain (see, e.g., [1]). This has motivated the development of Spiking Neural Networks (SNNs) as a low-power alternative to energy-hungry ANNs [2]. Unlike conventional ANNs, SNNs are trainable dynamic systems that make use of the temporal dimension, not just as a neutral substrate for computing, but as a means to encode and process information in the form of sparse spike signals. Proof-of-concept and commercial hardware implementations of SNNs have demonstrated orders-of-magnitude improvements in terms of energy efficiency over ANNs (see, e.g., [2] and references therein).

Deterministic vs probabilistic SNN models. The most common SNN model consists of a network of leaky integrate-and-fire neurons. Under this model, in a manner similar to ANNs, learning problems are typically formulated as the minimization of a loss function that measures the difference between a desired behavior of an output layer and the spike signals actually produced by such neurons. As for ANNs, this minimization requires backpropagation in order to carry out a credit assignment for the neurons in the intermediate layers. Unlike ANNs, however, backpropagation is made challenging by the non-differentiability of the output of the SNN with respect to the synaptic weights due to the threshold crossing-triggered spiking behavior. To obviate this problem, typical approaches approximate the derivative by smoothing out the membrane potential as a function of the weights [3]–[5].

In contrast to more conventional deterministic models for SNNs, a statistical signal processing formulation of the problem of training SNNs provides access to differentiable principled learning criteria from statistics and information theory, such as likelihood functions and mutual information. Furthermore, a probabilistic approach enables the modeling of more complex dependencies among the spiking behaviors of different neurons, as well as the derivation from first principles of many learning rules that have been proposed for SNNs in the computational neuroscience literature.

Scope and Overview. This paper aims at providing a review on the topic of probabilistic SNNs, by covering models, learning rules, and applications to supervised, unsupervised, and reinforcement learning from a stochastic signal processing viewpoint. The main goal is to make key ideas and tools used in this emerging field accessible to researchers in signal processing. These researchers may otherwise find it difficult to navigate the computational neuroscience literature on the subject given its focus on biological plausibility rather than theoretical and algorithmic principles. At the end of the paper, we also review extensions and open problems.

MODELS

In this section, we describe standard discrete-time models for multi-layer SNNs. Discrete-time models reflect the operation of a number of neuromorphic chips, including Intel's Loihi [2]. The focus on a

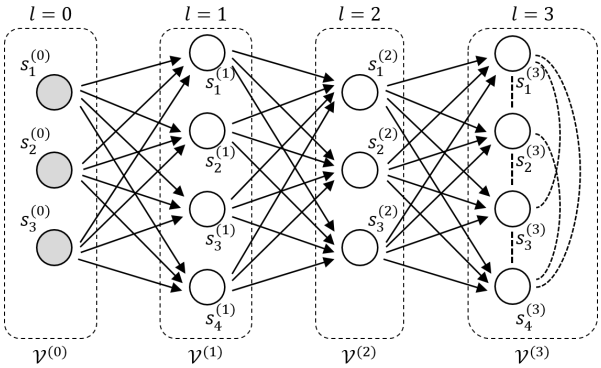

Fig. 1. An architecture of a four-layer SNN ($L = 3$) with $N^{(0)} = 3, N^{(1)} = 4, N^{(2)} = 3$, and $N^{(3)} = 4$ spiking neurons; the directed links (solid arrows) between two neurons in successive layers represent the causal feedforward, or synaptic, dependencies; and the undirected links (dashed lines) in layer 3 captures instantaneous correlations between neurons. In general, neurons in layer 1 or 2 may have undirected links between neurons in the same layer. Neurons in layer 0 (shaded) have fixed assigned spike signals that act as inputs to the SNN.

multi-layer architecture is also motivated by its practical relevance, although more general topologies are useful for a number of applications (see the section "Conclusions and Open Problems"). As we will see, models are defined by learnable parameters that can be adapted to carry out supervised, unsupervised, and reinforcement learning tasks.

Multi-layer topology. As illustrated in Fig. 1, a multi-layer SNN consists of $L + 1$ layers of spiking neurons, with the $N^{(l)}$ neurons in the lth layer being denoted as the set $\mathcal{V}^{(l)}$, for $l = 0, \ldots, L$. At any time $t = 1, 2, \ldots$, each neuron $i \in \mathcal{V}^{(l)}$ outputs a binary signal $s_{i,t}^{(l)} \in \{0, 1\}$, with value $s_{i,t}^{(l)} = 1$ corresponding to a *spike* emitted at time t. We collect in vector $\boldsymbol{s}_t^{(l)} = (s_{i,t}^{(l)} : i \in \mathcal{V}^{(l)})$ the binary signals emitted by all neurons in the lth layer at time t. Each neuron $i \in \mathcal{V}^{(l)}$ in layer l only receives the signals emitted by the neurons $\mathcal{V}^{(l-1)}$ in layer $l - 1$. The directed links between two neurons in successive layers are also known as *synapses*, and the neurons in layer $l - 1$ are referred to as *pre-synaptic* for *post-synaptic* neurons in layer l. The neurons $\mathcal{V}^{(0)}$ in layer 0 have fixed assigned signals $\boldsymbol{s}_t^{(0)}$, which act as inputs to the SNN. Therefore, we will focus on modeling the behavior of the neurons in layers $l = 1, \ldots, L$.

Membrane potential. The internal state of each spiking neuron $i \in \mathcal{V}^{(l)}$ in layer l at time t is defined by its *membrane potential* $u_{i,t}^{(l)}$ [6]. As we will see, a large membrane potential increases the probability of spiking. To elaborate, we denote as $\boldsymbol{s}_{i,\leq t}^{(l)} = (s_{i,1}^{(l)}, \ldots, s_{i,t}^{(l)})$ the spike signal emitted by neuron i in layer l up to time t, and as $\boldsymbol{s}_{\leq t}^{(l)} = (\boldsymbol{s}_1^{(l)}, \ldots, \boldsymbol{s}_t^{(l)})$ the collection of spike signals up to time t for all neurons in layer l. As illustrated in Fig. 2, given past input spike signals $\boldsymbol{s}_{\leq t-1}^{(l-1)}$ from the pre-synaptic neurons in layer $l - 1$ and the local spiking history $\boldsymbol{s}_{i,\leq t-1}^{(l)}$, the membrane potential of neuron i in the

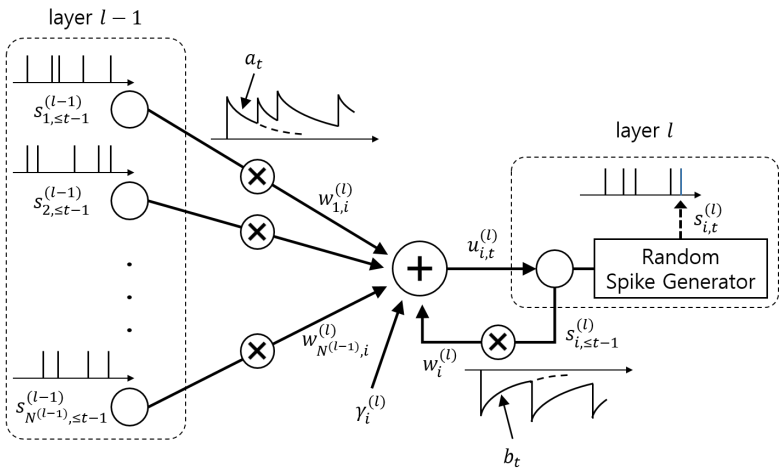

Fig. 2. Illustration of a membrane potential model with exponential feedforward and feedback kernels, see also Fig. 3. In presence of lateral connections, the operation of the random spike generator may be affected by other neurons in the same layer.

lth layer at time t can be written as [6]

$$u^{(l)}_{i,t} = \sum_{j\in\mathcal{V}^{(l-1)}} w^{(l)}_{j,i} \overrightarrow{s}^{(l-1)}_{j,t-1} + w^{(l)}_i \overleftarrow{s}^{(l)}_{i,t-1} + \gamma^{(l)}_i, \tag{1}$$

where the quantities $w^{(l)}_{j,i}$ for $j \in \mathcal{V}^{(l-1)}$ are synaptic (feedforward) weights; $w^{(l)}_i$ is a feedback weight; $\gamma^{(l)}_i$ is a bias parameter; and the quantities

$$\overrightarrow{s}^{(l)}_{i,t-1} = a_t * s^{(l)}_{i,t} \text{ and } \overleftarrow{s}^{(l)}_{i,t-1} = b_t * s^{(l)}_{i,t} \tag{2}$$

are known as *filtered feedforward and feedback traces* of neuron i, respectively, where $*$ denotes the convolution operator $f_t * g_t = \sum_{\delta\geq 1} f_\delta g_{t-\delta}$.

Kernels, weights, and filtered traces. In (1)-(2), the filter a_t defines the synaptic response to a spike from a pre-synaptic neuron at the post-synaptic neuron. This filter is known as the *feedforward, or synaptic, kernel*. A typical choice for the feedforward kernel is the function $a_t \propto \big(\exp(-t/\tau_1) - \exp(-t/\tau_2)\big)$ with time constants τ_1 and τ_2, as illustrated in Fig. 3. The filtered contribution of a spike from the pre-synaptic neuron $j \in \mathcal{V}^{(l-1)}$ is multiplied by a learnable weight $w^{(l)}_{j,i}$ for the synapse from neuron j to neuron $i \in \mathcal{V}^{(l)}$. The filter b_t describes the response of a neuron to a local spike, and is known as *feedback kernel*. A negative feedback kernel, such as $b_t \propto -\exp(-t/\tau_m)$ with time constant τ_m (see Fig. 3), can be used to model a refractory period upon the emission of a spike. As per (1), the filtered contribution of a local output spike is weighted by a learnable parameter $w^{(l)}_i$. We note that the duration of the feedforward kernel determines the synaptic memory and possible synaptic delays, while

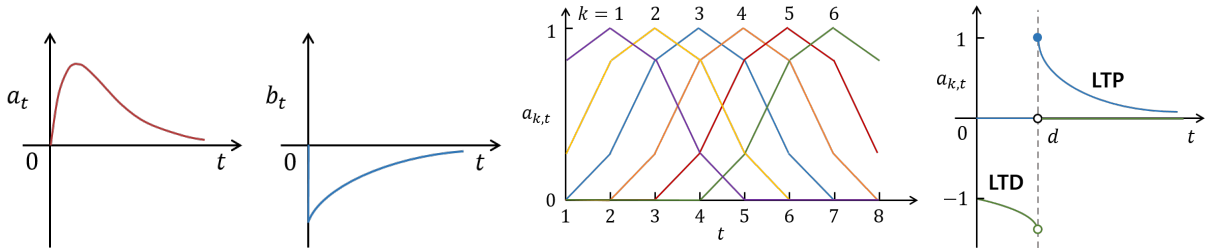

Fig. 3. Examples of feedforward/feedback kernels. From left to right: exponentially decaying feedforward kernel a_t; exponentially decaying feedback kernel b_t; raised cosine basis functions $a_{k,t}$ in [7]; and STDP basis functions $a_{k,t}$ for LTP (right, upper) and LTD (left, lower), where the synaptic conduction delay equals d [8].

the duration of the feedback kernel determines the refractory period.

More generally, a synapse can be associated with multiple learnable synaptic weights $\{w_{j,i,k}^{(l)}\}_{k=1}^{K_\alpha}$. In this case, the contribution from pre-synaptic neuron j in (1) can be written as [7]

$$\left(\sum_{k=1}^{K_\alpha} w_{j,i,k}^{(l)} a_{k,t}\right) * s_{j,t}^{(l)}, \tag{3}$$

where we have defined K_α fixed basis functions $\{a_{k,t}\}_{k=1}^{K_\alpha}$ with learnable weights $\{w_{j,i,k}^{(l)}\}_{k=1}^{K_\alpha}$. The feedback kernel can be similarly parameterized as the weighted sum of fixed K_β basis functions. Parameterization (3) makes it possible to adapt the filter applied by the synapse by learning the shape of the kernel functions through the weights $\{w_{j,i,k}^{(l)}\}_{k=1}^{K_\alpha}$. Examples of basis functions for feedforward kernels are provided in Fig. 3. In the rest of the paper, with the exception of the section "Applications", we focus on the simpler model (1)-(2).

Energy-based probabilistic model. The log-probability of desired spike signals $\boldsymbol{s}_{\leq T} = (\boldsymbol{s}_{\leq T}^{(1)}, \ldots, \boldsymbol{s}_{\leq T}^{(L)})$ emitted by all neurons in the SNN up to time T can be written according to the chain rule as

$$\log p_{\boldsymbol{\theta}}(\boldsymbol{s}_{\leq T}) = \sum_{t=1}^{T} \log p_{\boldsymbol{\theta}}(\boldsymbol{s}_t | \boldsymbol{s}_{\leq t-1}) = \sum_{l=1}^{L}\sum_{t=1}^{T} \log p_{\boldsymbol{\theta}^{(l)}}(\boldsymbol{s}_t^{(l)} | \boldsymbol{s}_{\leq t-1}^{(l-1)}, \boldsymbol{s}_{\leq t-1}^{(l)}). \tag{4}$$

The decomposition (4) is in terms of the conditional probabilities $p_{\boldsymbol{\theta}^{(l)}}(\boldsymbol{s}_t^{(l)} | \boldsymbol{s}_{\leq t-1}^{(l-1)}, \boldsymbol{s}_{\leq t-1}^{(l)})$, which represent the joint probability of spiking for the neurons at layer l given their past spike timings and the past behaviors of the neurons at layer $l-1$. The learnable parameter vector $\boldsymbol{\theta} = \{\boldsymbol{\theta}^{(l)}\}_{l=1}^{L}$ will be detailed below. Note that in (4), we have implicitly conditioned on spike values $\boldsymbol{s}_{\leq T}^{(0)}$ of the neurons in layer 0.

The conditional probabilities $p_{\boldsymbol{\theta}^{(l)}}(\boldsymbol{s}_t^{(l)} | \boldsymbol{s}_{\leq t-1}^{(l-1)}, \boldsymbol{s}_{\leq t-1}^{(l)})$ can capture two types of dependencies. The first is a causal dependence of the spiking behavior of each neuron $i \in \mathcal{V}^{(l)}$ on the history $(\boldsymbol{s}_{\leq t-1}^{(l-1)}, \boldsymbol{s}_{i,\leq t-1}^{(l)})$, which is mediated by the neuron's membrane potential $u_{i,t}^{(l)}$. The second is a pairwise correlation between

neurons in the same layer l, which either excites or inhibits the simultaneous spiking of the two neurons. Using an energy-based model, both dependencies are captured by joint distribution as [8]

$$p_{\boldsymbol{\theta}^{(l)}}(\boldsymbol{s}_t^{(l)}|\boldsymbol{s}_{\leq t-1}^{(l-1)}, \boldsymbol{s}_{\leq t-1}^{(l)}) = p_{\boldsymbol{r}^{(l)}}(\boldsymbol{s}_t^{(l)}|\boldsymbol{u}_t^{(l)}) \tag{5a}$$

$$\propto \exp\left\{ \sum_{i\in\mathcal{V}^{(l)}} u_{i,t}^{(l)} s_{i,t}^{(l)} + \sum_{i,j\in\mathcal{V}^{(l)}} r_{i,j}^{(l)} s_{i,t}^{(l)} s_{j,t}^{(l)} \right\}, \tag{5b}$$

where $\boldsymbol{u}_t^{(l)} = (u_{i,t}^{(l)} : i \in \mathcal{V}^{(l)})$ contains the membrane potentials (1) for all neurons $\mathcal{V}^{(l)}$ at time t and the second sum in (5b) is taken over all pairs of neurons in $\mathcal{V}^{(l)}$. In (5b), the first term describes the causal feedforward and feedback dependencies of the spike signals for layer l: the larger the potential $u_{i,t}^{(l)}$ is, the more likely it is that neuron i spikes, i.e., that we have $s_{i,t}^{(l)} = 1$. In contrast, the lateral correlations between neurons in the same lth layer are defined by parameters $\boldsymbol{r}^{(l)} = \{r_{i,j}^{(l)}\}_{i,j\in\mathcal{V}^{(l)}}$. A positive value of $r_{i,j}^{(l)}$ encourages the simultaneous spiking of the neurons i and j in layer l; while a negative value of $r_{i,j}^{(l)}$ hinders the emission of simultaneous spikes by the two neurons. This enables forms of population coding, such as the Winner-Take-All (WTA) circuit [9] (see the box "Spike-Domain Coding and Decoding").

The model (5) is parameterized by the learnable vector $\boldsymbol{\theta}^{(l)} = \{\boldsymbol{\theta}_i^{(l)}\}_{i\in\mathcal{V}^{(l)}}$, where we denote by $\boldsymbol{\theta}_i^{(l)} = \{\gamma_i^{(l)}, \{w_{j,i}^{(l)}\}_{j\in\mathcal{V}^{(l-1)}}, w_i^{(l)}, \{r_{i,j}^{(l)}\}_{j\in\mathcal{V}^{(l)}}\}$ the local parameters of neuron i in the lth layer. Furthermore, as indicated by the right-hand-side of (5a), when conditioning on the membrane potentials $\boldsymbol{u}_t^{(l)}$, the probability only depends on the learnable parameters $\boldsymbol{r}^{(l)}$.

Generalized Linear Model (GLM). Due to lateral correlations between neurons, the conditional probability (5) cannot be generally decomposed into the firing probabilities for each individual neuron in layer l. However, if there are no lateral connections, i.e., if $\boldsymbol{r}^{(l)} = \mathbf{0}$, the outputs of the neurons in layer l are conditionally independent. This yields the Generalized Linear Model (GLM), also known as Spike Response Model with escape noise [6]. According to this model, we have the factorization

$$p_{\boldsymbol{\theta}}(\boldsymbol{s}_t|\boldsymbol{s}_{\leq t-1}) = p(\boldsymbol{s}_t|\boldsymbol{u}_t) = \prod_{l=1}^{L} \prod_{i\in\mathcal{V}^{(l)}} p(s_{i,t}^{(l)}|u_{i,t}^{(l)}), \tag{6}$$

where the instantaneous firing rate of neuron $i \in \mathcal{V}^{(l)}$ at time t is equal to

$$p(s_{i,t}^{(l)} = 1|u_{i,t}^{(l)}) = \sigma(u_{i,t}^{(l)}), \tag{7}$$

with $\sigma(\cdot)$ being the sigmoid function, i.e., $\sigma(x) = 1/(1+\exp(-x))$. In a variant of this model, probability (7) can be written as $\sigma(u_{i,t}^{(l)}/\Delta u)$, where Δu is a "bandwidth" parameter that dictates the smoothness of the firing rate about the threshold. When taking the limit $\Delta u \to 0$, this variant of GLM reduces to the deterministic leaky integrate-and-fire model [10].

Gradient of the log-likelihood. The gradient of the log-probability, or *log-likelihood*, $\mathcal{L}_{\boldsymbol{s}_{\leq T}}(\boldsymbol{\theta}) = \log p_{\boldsymbol{\theta}}(\boldsymbol{s}_{\leq T})$ in (4) with respect to the learnable parameters $\boldsymbol{\theta}$ plays a key role in the problem of training a probabilistic SNN. Focusing on any neuron $i \in \mathcal{V}^{(l)}$, from (1)-(5), the gradient of the log-likelihood with respect to the local parameters $\boldsymbol{\theta}_i^{(l)}$ is given as $\nabla_{\boldsymbol{\theta}_i^{(l)}} \mathcal{L}_{\boldsymbol{s}_{\leq T}}(\boldsymbol{\theta}) = \sum_{t=1}^{T} \nabla_{\boldsymbol{\theta}_i^{(l)}} \log p_{\boldsymbol{\theta}}(\boldsymbol{s}_t | \boldsymbol{s}_{\leq t-1})$, where the contribution to the gradient of time t can be obtained as

$$\nabla_{\gamma_i^{(l)}} \log p_{\boldsymbol{\theta}}(\boldsymbol{s}_t | \boldsymbol{s}_{\leq t-1}) = s_{i,t}^{(l)} - p_{\boldsymbol{r}^{(l)}}\big(s_{i,t}^{(l)} = 1 | \boldsymbol{u}_t^{(l)}\big), \tag{8a}$$

$$\nabla_{w_{j,i}^{(l)}} \log p_{\boldsymbol{\theta}}(\boldsymbol{s}_t | \boldsymbol{s}_{\leq t-1}) = \overrightarrow{s}_{j,t-1}^{(l-1)} \Big(s_{i,t}^{(l)} - p_{\boldsymbol{r}^{(l)}}\big(s_{i,t}^{(l)} = 1 | \boldsymbol{u}_t^{(l)}\big) \Big), \tag{8b}$$

$$\nabla_{w_i^{(l)}} \log p_{\boldsymbol{\theta}}(\boldsymbol{s}_t | \boldsymbol{s}_{\leq t-1}) = \overleftarrow{s}_{i,t-1}^{(l)} \Big(s_{i,t}^{(l)} - p_{\boldsymbol{r}^{(l)}}\big(s_{i,t}^{(l)} = 1 | \boldsymbol{u}_t^{(l)}\big) \Big), \tag{8c}$$

$$\text{and} \quad \nabla_{r_{i,j}^{(l)}} \log p_{\boldsymbol{\theta}}(\boldsymbol{s}_t | \boldsymbol{s}_{\leq t-1}) = s_{i,t}^{(l)} s_{j,t}^{(l)} - p_{\boldsymbol{r}^{(l)}}\big(s_{i,t}^{(l)} s_{j,t}^{(l)} = 1 | \boldsymbol{u}_t^{(l)}\big). \tag{8d}$$

The gradients (8) depend on the difference between the desired spiking behavior and its average behavior under the model distribution (5). Note that, if there are no lateral connections, from (6), the marginal probability $p_{\boldsymbol{r}^{(l)}}(s_{i,t}^{(l)} = 1 | \boldsymbol{u}_t^{(l)})$ is equal to (7). Further discussion will be provided in the next section.

On implementation. In a hardware implementation, randomness in spiking behavior can be obtained via pseudo-random number generators, such as linear feedback shift registers [6]. Randomness may, however, also be caused by extrinsic factors, such as random inputs, fluctuating currents, or inputs from other SNNs [11].

SPIKE-DOMAIN CODING AND DECODING

Neural coding describes the transformation of an input stimulus into a spiking form that is appropriate for processing by an SNN. Neural decoding is instead concerned with extracting features of spike signals that provide an interpretable output to the end user, such as an actuator. Various coding and decoding strategies have been discussed in the neuro-computational literature, each with their own strengths and limitations depending on the problem domain. A short review is provided in this box.

With rate-based coding, the magnitude of an input is encoded into the spiking frequency of spike signals by using either deterministic or random, such as Poisson, mechanisms [1]. A limitation of rate-based coding is that a reliable estimate of a neuron's firing rate may require long observation windows. Temporal coding and decoding are instead based on the precise timings of spikes [12]. Single-spike techniques encode information in the time of the first spike of a neuron, while multi-spike methods encode information in the sequence of the inter-spike timings. For example, an

analog time signal can be encoded by firing a spike as soon as the variation from the previously encoded signal exceeds a threshold [13]. By comparison with rate-coding, temporal coding can carry more information within a given interval of time, but it may be more susceptible to noise, particularly for single-spike methods.

Rank-order coding encodes information in the order in which a set of neurons respond with their first spikes, hence discarding the neurons' subsequent firing times [12]. Generalizing rank-order coding, population coding carries information in the joint spiking behavior of a group of neurons. A key advantage to population coding is that it can potentially reduce the detrimental impact of noise on individual neurons [14]. Population decoding techniques are often used. For example, for classification problems, the output class can be selected by choosing the index of the neuron in the output layer that has the largest spiking frequency as in a WTA circuit [9] or that spikes first as in first-to-spike decoding [6].

TRAINING SNNS

SNNs can be used to carry out supervised, unsupervised, and reinforcement learning tasks. To this end, the network follows a *learning rule*, which defines how the model parameters $\boldsymbol{\theta}$ are updated on the basis of the available observations. Learning rules can be applied in an *on-line* fashion, i.e., after each time instant t; periodically [2]; or in a *batch* mode at the end of a full period T of use of the SNN.

Locality. A learning rule is *local* if its operation can be decomposed into atomic steps that can be carried out in parallel at distributed processors based only on locally available information and limited communication on the connectivity graph (see Fig. 1). Local information that can be communicated among processors generally includes the membrane potentials, the filtered traces, and the model parameters. The processors will be considered here to be conventionally implemented at the level of individual neurons. Beside local signals, learning rules may also require global feedback signals, as discussed next.

Three-factor rule. While the details differ for each learning rule and learning task, a general form of the learning rule for the synaptic weights follows the *three-factor* rule [15], [16]. Accordingly, the synaptic weight $w_{j,i}^{(l)}$ from pre-synaptic neuron $j \in \mathcal{V}^{(l-1)}$ to a post-synaptic neuron $i \in \mathcal{V}^{(l)}$ is updated as

$$w_{j,i}^{(l)} \leftarrow w_{j,i}^{(l)} + \eta \times \ell \times \text{pre}_j \times \text{post}_i, \tag{9}$$

where η is a learning rate; ℓ is a scalar *global learning signal* that determines sign and magnitude of the update; the term "pre_j" is a function of the activity of the pre-synaptic neuron $j \in \mathcal{V}^{(l-1)}$; and the

term "post$_i$" depends on the activity of the post-synaptic neuron $i \in \mathcal{V}^{(l)}$. For most learning rules, pre- and post-synaptic terms are local to each neuron, while the learning signal ℓ, if present, plays the role of a global feedback signal, which is also known as neuromodulator in neuroscience. The rule (9) can implement Hebb's hypothesis that "neurons that spike together wire together". This is done by ensuring that the product of "pre$_j$" and "post$_i$" terms is large when the two neurons spike at nearly the same time, resulting in a large change of the synaptic weight $w_{j,i}^{(l)}$.

In the next two sections, we will see how learning rules of the form (9) can be derived in a principled manner as stochastic gradient descent (SGD) updates obtained under the described probabilistic SNN models. We will also discuss how to update all other learnable parameters $\boldsymbol{\theta}$.

TRAINING SNNS: FULLY OBSERVED MODELS

In this section and in the next, we discuss the problem of learning the parameters of a probabilistic SNN. We first cover in this section the case of fully observed spike signals, while the more complex scenario with latent or hidden neurons is presented in the next section.

Fully observed vs partially observed models. In the case of *fully observed models*, the data specifies a desired spiking behavior for all neurons. For example, as we will detail in the section "Applications", in a two-layer SNN ($L = 1$) used for classification (supervised learning), the training set typically specifies both the input and the desired output spike signals at layer 0 and 1, respectively, once a coding and decoding technique is fixed (see the box "Spike-Domain Coding and Decoding"). In contrast, in the case of *partially observed models*, the training set only defines the desired spiking behavior of a subset of neurons, while leaving that of so-called *latent, or hidden, neurons* undefined. Examples of partially observed models include classification in multi-layer networks with intermediate, hidden, layers, i.e., with $L > 1$.

Maximum Likelihood Learning via Stochastic Gradient Descent

The standard learning criterion for probabilistic models is Maximum Likelihood (ML). ML selects model parameters that maximize the probability of the observed data under the model, also known as likelihood. In the set-up considered here, any example in the training set $\mathcal{D} = \{\boldsymbol{x}_{\leq T}^m\}_{m=1}^M$ of M examples consists of fully observed spike signals $\boldsymbol{x}_{\leq T}^m$ for all the neurons in the SNN. Using the notation in the previous section, we hence have $\boldsymbol{s}_{\leq T} = \boldsymbol{x}_{\leq T}^m$ for all examples m. During each iteration of training, the spike signals for all neurons are hence "clamped" to the values assumed in some data point $\boldsymbol{x}_{\leq T}^m = \boldsymbol{x}_{\leq T} \in \mathcal{D}$. The log-likelihood for any example $\boldsymbol{x}_{\leq T} \in \mathcal{D}$ is given as $\mathcal{L}_{\boldsymbol{x}_{\leq T}}(\boldsymbol{\theta}) = \log p_{\boldsymbol{\theta}}(\boldsymbol{x}_{\leq T})$ in (4) with $\boldsymbol{s}_{\leq T} = \boldsymbol{x}_{\leq T}$.

Algorithm 1: ML Training via Batch SGD

Input: Training set $\mathcal{D} = \{\boldsymbol{x}_{\leq T}^m\}_{m=1}^M$ and learning rate η
Output: Learned model parameters $\boldsymbol{\theta}$

initialize parameters $\boldsymbol{\theta}$
repeat
  draw an example $\boldsymbol{x}_{\leq T}$ from the training set $\mathcal{D}$
  for each neuron $i \in \mathcal{V}^{(l)}$ for all layers $l = 1, \ldots, L$ **do**
    compute the gradient $\nabla_{\boldsymbol{\theta}_i^{(l)}} \mathcal{L}_{\boldsymbol{x}_{\leq T}}(\boldsymbol{\theta}) = \sum_{t=1}^T \nabla_{\boldsymbol{\theta}_i^{(l)}} \log p_{\boldsymbol{\theta}}(\boldsymbol{x}_t | \boldsymbol{x}_{\leq t-1})$ with respect to the local parameters $\boldsymbol{\theta}_i^{(l)}$ from (8a)-(8d)
  end
  update model parameters

$$\boldsymbol{\theta} \leftarrow \boldsymbol{\theta} + \eta \nabla_{\boldsymbol{\theta}} \mathcal{L}_{\boldsymbol{x}_{\leq T}}(\boldsymbol{\theta}) \tag{10}$$

until stopping criterion is satisfied

Stochastic Gradient Descent (SGD). SGD yields efficient learning rules that are the workhorse of machine learning via ANNs (see, e.g., [17]). At each iteration, as summarized in Algorithm 1, the SGD-based rule considers one example $\boldsymbol{x}_{\leq T}$ from the training set, and updates the model parameters $\boldsymbol{\theta}$ in the direction of the gradient $\nabla_{\boldsymbol{\theta}} \mathcal{L}_{\boldsymbol{x}_{\leq T}}(\boldsymbol{\theta}) = \sum_{t=1}^T \nabla_{\boldsymbol{\theta}} \log p_{\boldsymbol{\theta}}(\boldsymbol{x}_t | \boldsymbol{x}_{\leq t-1})$ in (8). The algorithm can be generalized by summing over a minibatch of examples from the training set at each iteration. The update (10) in Algorithm 1 is applied at the end of the observation period T and is hence a batch rule. It is also possible to obtain an on-line version of the rule by substituting (10) with the update $\boldsymbol{\theta} \leftarrow \boldsymbol{\theta} + \eta \boldsymbol{e}_t$, applied at each time t, where the so-called eligibility trace $\boldsymbol{e}_t$ is a filtered version of the gradients evaluated so far [10], [16].

Interpretation. The learning rule (10) applies the gradients (8) to all model parameters. We first consider the update for the synaptic weights in light of the general rule (9). The gradient (8b) for any synaptic weight $w_{j,i}^{(l)}$ yields a *two-factor* learning rule, whereby the global learning signal is absent; the pre-synaptic term is given by the filtered feedforward trace $\overrightarrow{x}_{j,t-1}^{(l-1)}$ of neuron j; and the post-synaptic term is given by the error term $x_{i,t}^{(l)} - p_{\boldsymbol{r}^{(l)}}(x_{i,t}^{(l)} = 1 | \boldsymbol{u}_t^{(l)})$. This measures the difference between the desired spiking behavior of the neuron i at any time t and its average behavior under the model distribution (5). This two-factor rule is in line with the standard Spiking-Timing Dependent Plasticity (STDP) rule [8], [18]–[20], which stipulates that Long-Term Potentiation (LTP) of a synapse occurs when the pre-synaptic neuron spikes right before a post-synaptic neuron, while Long-Term Depression (LTD) of a synapse takes place when the pre-synaptic neuron spikes right after a post-synaptic neuron. In fact, with the basis functions depicted in the rightmost part of Fig. 3, if a pre-synaptic spike occurs more than d steps prior

to the post-synaptic spike at time t, an increase in the synaptic weight, or LTP, occurs, while a decrease in the synaptic weight, or LTD, takes place otherwise [8]. The parameter d can hence be interpreted as synaptic delay.

All other gradients (8) also depend on an error signal measuring the gap between desired and average model behavior. In (8a)-(8c), the desired behavior is given by samples $s_{i,t}^{(l)} = x_{i,t}^{(l)}$ in the training example, while (8d) specifies the desired correlation between two neurons in the same layer. The contribution of this error signal can be interpreted as a form of *homeostatic plasticity* [21] in that it regulates the neuronal firing rates around desirable set-point values.

Locality and implementation. Given the absence of a global learning signal, the SGD rule in Algorithm 1 can be implemented locally, so that each neuron i in layer l updates its own local parameters $\boldsymbol{\theta}_i^{(l)}$. To see how this can be done, consider first the case of no lateral edges, i.e., $\boldsymbol{r}^{(l)} = \mathbf{0}$. Under this assumption, each neuron $i \in \mathcal{V}^{(l)}$ uses information about the local spike signal $x_{i,t}^{(l)}$, the feedforward filtered traces $\overrightarrow{x}_{j,t-1}^{(l-1)}$ for all pre-synaptic neurons $j \in \mathcal{V}^{(l-1)}$, and the local feedback filtered trace $\overleftarrow{x}_{i,t-1}^{(l)}$ in order to compute the first terms in (8a)-(8c), while the second terms in (8a)-(8c) are obtained from (7).

If there are lateral connections, each neuron $i \in \mathcal{V}^{(l)}$ also needs information about the desired behavior of the spike signals $x_{j,t}^{(l)}$ of all neurons j in the layer l in order to compute the first term in (8d), as well as the membrane potentials $\boldsymbol{u}_t^{(l)}$ of all neurons in the same layer so as to compute the marginal probability (5) for the second terms in (8). This marginalization can be carried out efficiently by using Monte Carlo methods such as Gibbs sampling and Contrastive Divergence [17], [22], [23].

TRAINING SNNS: PARTIALLY OBSERVED MODELS

In this section, we consider an SNN whose spiking behavior is only partially specified in the training set. As we will see in the section "Applications", this more general set-up arises in important problems for supervised and unsupervised learning with multi-layer SNNs.

Latent neurons. Focusing on any layer l of a multi-layer probabilistic SNN in the "Models" section, the set $\mathcal{V}^{(l)}$ of neurons is assumed to be partitioned into disjoint subsets of observed and hidden neurons. The $N_{\mathrm{X}}^{(l)}$ neurons in the subset $\mathcal{X}^{(l)}$ are observed, and the $N_{\mathrm{H}}^{(l)}$ neurons in the subset $\mathcal{H}^{(l)}$ are hidden, or latent, and we have $\mathcal{V}^{(l)} = \mathcal{X}^{(l)} \cup \mathcal{H}^{(l)}$. We write as $\boldsymbol{x}_t^{(l)} = (x_{i,t}^{(l)} : i \in \mathcal{X}^{(l)})$ and $\boldsymbol{h}_t^{(l)} = (h_{i,t}^{(l)} : i \in \mathcal{H}^{(l)})$ the binary signals emitted by the observed and hidden neurons in the lth layer at time t, respectively. Therefore, using the notation in the "Models" section, we have $s_{i,t}^{(l)} = x_{i,t}^{(l)}$ for any observed neuron $i \in \mathcal{X}^{(l)}$ and $s_{i,t}^{(l)} = h_{i,t}^{(l)}$ for any latent neuron $i \in \mathcal{H}^{(l)}$, as well as $\boldsymbol{s}_t^{(l)} = (\boldsymbol{x}_t^{(l)}, \boldsymbol{h}_t^{(l)})$ for the overall set of spike signals at layer l. The training set $\mathcal{D} = \{\boldsymbol{x}_{\leq T}^m\}_{m=1}^M$ includes only M samples of the observed

spike signals $\boldsymbol{x}_{\leq T}^m$, while the spike signals $\boldsymbol{h}_{\leq T}^m$ are not available. Therefore, during training, only the spike signals of the observed neurons are clamped to the examples in the training set.

Joint probability distribution. Mathematically, the probabilistic model is defined as in (4)-(5) with $\boldsymbol{s}_{\leq T} = (\boldsymbol{x}_{\leq T}, \boldsymbol{h}_{\leq T})$. In this section, in order to simplify the derivation and the resulting learning rules, we assume that only the observed neurons in the same layer may have lateral connections. This is similar to the assumption made in [24] and captures important practical scenarios such as multi-task supervised learning problems with correlated output neurons (see the "Applications" section). According to this model, due to the absence of lateral connections between observed and hidden neurons, we have the factorization

$$p_{\boldsymbol{\theta}}(\boldsymbol{x}_t, \boldsymbol{h}_t | \boldsymbol{x}_{\leq t-1}, \boldsymbol{h}_{\leq t-1}) = p_{\boldsymbol{\theta}^{\mathrm{X}}}(\boldsymbol{x}_t | \boldsymbol{x}_{\leq t-1}, \boldsymbol{h}_{\leq t-1}) \cdot p_{\boldsymbol{\theta}^{\mathrm{H}}}(\boldsymbol{h}_t | \boldsymbol{x}_{\leq t-1}, \boldsymbol{h}_{\leq t-1}), \tag{11}$$

where the model parameters $\boldsymbol{\theta}$ are also decomposed into disjoint sets $\boldsymbol{\theta}^{\mathrm{X}} = \{\{\boldsymbol{\theta}_i^{(l)}\}_{i \in \mathcal{X}^{(l)}}\}_{l=1}^L$ and $\boldsymbol{\theta}^{\mathrm{H}} = \{\{\boldsymbol{\theta}_i^{(l)}\}_{i \in \mathcal{H}^{(l)}}\}_{l=1}^L$ for observed and hidden neurons, respectively. Note that we have $\boldsymbol{\theta} = \boldsymbol{\theta}^{\mathrm{X}} \cup \boldsymbol{\theta}^{\mathrm{H}}$, and that only observed neurons $i \in \mathcal{X}^{(l)}$ have lateral correlation parameters $\{r_{i,j}^{(l)}\}_{j \in \mathcal{X}^{(l)}}$ in vector $\boldsymbol{\theta}_i^{(l)}$.

Maximum Likelihood via Stochastic Gradient Descent and Variational Learning

In this section, we review a learning rule that tackles the ML problem by using SGD and variational learning. Unlike in the fully observed case, as we will see, variational learning is needed in order to cope with the complexity of computing the gradient of the log-likelihood of the observed spike signals in the presence of hidden variables [23].

Log-likelihood. The log-likelihood of any example of observed spike signals $\boldsymbol{x}_{\leq T} \in \mathcal{D}$ in the training set is obtained via marginalization by summing over all possible values of the latent spike signals $\boldsymbol{h}_{\leq T}$ as $\mathcal{L}_{\boldsymbol{x}_{\leq T}}(\boldsymbol{\theta}) = \log p_{\boldsymbol{\theta}}(\boldsymbol{x}_{\leq T}) = \log \sum_{\boldsymbol{h}_{\leq T}} p_{\boldsymbol{\theta}}(\boldsymbol{x}_{\leq T}, \boldsymbol{h}_{\leq T})$. Let us denote as $\langle \cdot \rangle_p$ the expectation over a distribution p as in $\langle f(x) \rangle_{p(x)} = \sum_x f(x) p(x)$, for some function $f(x)$. The gradient of the log-likelihood with respect to the model parameters $\boldsymbol{\theta}$ can be expressed as (see, e.g., [23, Ch. 6])

$$\nabla_{\boldsymbol{\theta}} \mathcal{L}_{\boldsymbol{x}_{\leq T}}(\boldsymbol{\theta}) = \Big\langle \nabla_{\boldsymbol{\theta}} \log p_{\boldsymbol{\theta}}(\boldsymbol{x}_{\leq T}, \boldsymbol{h}_{\leq T}) \Big\rangle_{p_{\boldsymbol{\theta}}(\boldsymbol{h}_{\leq T} | \boldsymbol{x}_{\leq T})}, \tag{12}$$

where the expectation is with respect to the posterior distribution $p_{\boldsymbol{\theta}}(\boldsymbol{h}_{\leq T} | \boldsymbol{x}_{\leq T})$ of the latent variables $\boldsymbol{h}_{\leq T}$ given the observation $\boldsymbol{x}_{\leq T}$. Note that the gradient $\nabla_{\boldsymbol{\theta}} \log p_{\boldsymbol{\theta}}(\boldsymbol{x}_{\leq T}, \boldsymbol{h}_{\leq T}) = \sum_{t=1}^T \nabla_{\boldsymbol{\theta}} \log p_{\boldsymbol{\theta}}(\boldsymbol{x}_t, \boldsymbol{h}_t | \boldsymbol{x}_{\leq t-1}, \boldsymbol{h}_{\leq t-1})$ is obtained from (8) with $\boldsymbol{s}_{\leq T} = (\boldsymbol{x}_{\leq T}, \boldsymbol{h}_{\leq T})$. Computing the posterior $p_{\boldsymbol{\theta}}(\boldsymbol{h}_{\leq T} | \boldsymbol{x}_{\leq T})$ amounts to the Bayesian inference of the hidden spike signals for the observed values $\boldsymbol{x}_{\leq T}$. Given that we have the equality $p_{\boldsymbol{\theta}}(\boldsymbol{h}_{\leq T} | \boldsymbol{x}_{\leq T}) = p_{\boldsymbol{\theta}}(\boldsymbol{x}_{\leq T}, \boldsymbol{h}_{\leq T}) / p_{\boldsymbol{\theta}}(\boldsymbol{x}_{\leq T})$, this task requires the evaluation of the marginal dis-

tribution $p_{\boldsymbol{\theta}}(\boldsymbol{x}_{\leq T}) = \sum_{\boldsymbol{h}_{\leq T}} p_{\boldsymbol{\theta}}(\boldsymbol{x}_{\leq T}, \boldsymbol{h}_{\leq T})$. For problems of practical size, this computation is intractable and hence so is evaluating the gradient (12).

Variational learning. Variational learning approximates the true posterior distribution $p_{\boldsymbol{\theta}}(\boldsymbol{h}_{\leq T}|\boldsymbol{x}_{\leq T})$ by means of any arbitrary *variational posterior* distribution $q_{\boldsymbol{\phi}}(\boldsymbol{h}_{\leq T}|\boldsymbol{x}_{\leq T})$ parameterized by a vector $\boldsymbol{\phi}$ of learnable parameters. For any variational distribution $q_{\boldsymbol{\phi}}(\boldsymbol{h}_{\leq T}|\boldsymbol{x}_{\leq T})$, using Jensen's inequality, the log-likelihood $\mathcal{L}_{\boldsymbol{x}_{\leq T}}(\boldsymbol{\theta})$ can be lower bounded as (see, e.g., [23, Ch. 6 and Ch. 8])

$$\begin{aligned}\mathcal{L}_{\boldsymbol{x}_{\leq T}}(\boldsymbol{\theta}) = \log \sum_{\boldsymbol{h}_{\leq T}} p_{\boldsymbol{\theta}}(\boldsymbol{x}_{\leq T}, \boldsymbol{h}_{\leq T}) &\geq \sum_{\boldsymbol{h}_{\leq T}} q_{\boldsymbol{\phi}}(\boldsymbol{h}_{\leq T}|\boldsymbol{x}_{\leq T}) \log \frac{p_{\boldsymbol{\theta}}(\boldsymbol{x}_{\leq T}, \boldsymbol{h}_{\leq T})}{q_{\boldsymbol{\phi}}(\boldsymbol{h}_{\leq T}|\boldsymbol{x}_{\leq T})} \\ &= \Big\langle \ell_{\boldsymbol{\theta},\boldsymbol{\phi}}\big(\boldsymbol{x}_{\leq T}, \boldsymbol{h}_{\leq T}\big) \Big\rangle_{q_{\boldsymbol{\phi}}(\boldsymbol{h}_{\leq T}|\boldsymbol{x}_{\leq T})} := L_{\boldsymbol{x}_{\leq T}}(\boldsymbol{\theta}, \boldsymbol{\phi}), \end{aligned} \tag{13}$$

where we have defined the *learning signal* as

$$\ell_{\boldsymbol{\theta},\boldsymbol{\phi}}(\boldsymbol{x}_{\leq T}, \boldsymbol{h}_{\leq T}) := \log p_{\boldsymbol{\theta}}(\boldsymbol{x}_{\leq T}, \boldsymbol{h}_{\leq T}) - \log q_{\boldsymbol{\phi}}(\boldsymbol{h}_{\leq T}|\boldsymbol{x}_{\leq T}). \tag{14}$$

A baseline variational learning rule, also known as variational Expectation Maximization (EM) algorithm, is based on the maximization of the Evidence Lower BOund (ELBO) $L_{\boldsymbol{x}_{\leq T}}(\boldsymbol{\theta}, \boldsymbol{\phi})$ in (13) with respect to both the model parameters $\boldsymbol{\theta}$ and the variational parameters $\boldsymbol{\phi}$. Accordingly, for a given observed example $\boldsymbol{x}_{\leq T} \in \mathcal{D}$, the learning rule is given by gradient ascent updates, where the gradients can be computed as

$$\nabla_{\boldsymbol{\theta}} L_{\boldsymbol{x}_{\leq T}}(\boldsymbol{\theta}, \boldsymbol{\phi}) = \Big\langle \nabla_{\boldsymbol{\theta}} \log p_{\boldsymbol{\theta}}(\boldsymbol{x}_{\leq T}, \boldsymbol{h}_{\leq T}) \Big\rangle_{q_{\boldsymbol{\phi}}(\boldsymbol{h}_{\leq T}|\boldsymbol{x}_{\leq T})}, \text{ and} \tag{15a}$$

$$\nabla_{\boldsymbol{\phi}} L_{\boldsymbol{x}_{\leq T}}(\boldsymbol{\theta}, \boldsymbol{\phi}) = \Big\langle \ell_{\boldsymbol{\theta},\boldsymbol{\phi}}(\boldsymbol{x}_{\leq T}, \boldsymbol{h}_{\leq T}) \cdot \nabla_{\boldsymbol{\phi}} \log q_{\boldsymbol{\phi}}(\boldsymbol{h}_{\leq T}|\boldsymbol{x}_{\leq T}) \Big\rangle_{q_{\boldsymbol{\phi}}(\boldsymbol{h}_{\leq T}|\boldsymbol{x}_{\leq T})}, \tag{15b}$$

respectively. The gradient (15a) is derived in a manner analogous to (12), and the gradient (15b) is obtained from the standard REINFORCE, or score function, gradient [23, Ch. 8], [25]. Importantly, the gradients (15) require expectations with respect to the known variational posterior $q_{\boldsymbol{\phi}}(\boldsymbol{h}_{\leq T}|\boldsymbol{x}_{\leq T})$ evaluated at the current value of variational parameters $\boldsymbol{\phi}$ rather than with respect to the hard-to-compute posterior $p_{\boldsymbol{\theta}}(\boldsymbol{h}_{\leq T}|\boldsymbol{x}_{\leq T})$.

In practice, computing the averages in (15) is still intractable due to the large domain of the hidden variables $\boldsymbol{h}_{\leq T}$. Therefore, the expectations over the the variational posterior are typically approximated by means of Monte Carlo empirical averages. This is possible as long as sampling from the variational posterior $q_{\boldsymbol{\phi}}(\boldsymbol{h}_{\leq T}|\boldsymbol{x}_{\leq T})$ is feasible. As an example, if a single spike signals $\hat{\boldsymbol{h}}_{\leq T}$ is sampled from

Algorithm 2: ML Training via Batch Doubly SGD and Variational Learning

Input: Training set $\mathcal{D} = \{\boldsymbol{x}_{\leq T}^m\}_{m=1}^M$ and learning rates $\eta_{\boldsymbol{\theta}}$ and $\eta_{\boldsymbol{\phi}}$
Output: Learned model parameters $\boldsymbol{\theta}$ and variational parameters $\boldsymbol{\phi}$

initialize parameters $\boldsymbol{\theta}$ and $\boldsymbol{\phi}$
repeat
  draw an example $\boldsymbol{x}_{\leq T}$ from the training set $\mathcal{D}$
  draw a sample of latent spike signals $\hat{\boldsymbol{h}}_{\leq T}$ from the variational posterior $q_{\boldsymbol{\phi}}(\boldsymbol{h}_{\leq T}|\boldsymbol{x}_{\leq T})$
  compute the gradients $\nabla_{\boldsymbol{\theta}} \hat{L}_{\boldsymbol{x}_{\leq T}}(\boldsymbol{\theta}, \boldsymbol{\phi})$ in (16a) and $\nabla_{\boldsymbol{\phi}} \hat{L}_{\boldsymbol{x}_{\leq T}}(\boldsymbol{\theta}, \boldsymbol{\phi})$ in (16b)
  update model parameters and variational parameters

$$\boldsymbol{\theta} \leftarrow \boldsymbol{\theta} + \eta_{\boldsymbol{\theta}} \nabla_{\boldsymbol{\theta}} \hat{L}_{\boldsymbol{x}_{\leq T}}(\boldsymbol{\theta}, \boldsymbol{\phi}), \text{ and} \tag{17a}$$

$$\boldsymbol{\phi} \leftarrow \boldsymbol{\phi} + \eta_{\boldsymbol{\phi}} \nabla_{\boldsymbol{\phi}} \hat{L}_{\boldsymbol{x}_{\leq T}}(\boldsymbol{\theta}, \boldsymbol{\phi}) \tag{17b}$$

until stopping criterion is satisfied

$q_{\boldsymbol{\phi}}(\boldsymbol{h}_{\leq T}|\boldsymbol{x}_{\leq T})$, we obtain the Monte Carlo approximations of (15) as

$$\nabla_{\boldsymbol{\theta}} \hat{L}_{\boldsymbol{x}_{\leq T}}(\boldsymbol{\theta}, \boldsymbol{\phi}) = \nabla_{\boldsymbol{\theta}} \log p_{\boldsymbol{\theta}}(\boldsymbol{x}_{\leq T}, \hat{\boldsymbol{h}}_{\leq T}), \text{ and} \tag{16a}$$

$$\nabla_{\boldsymbol{\phi}} \hat{L}_{\boldsymbol{x}_{\leq T}}(\boldsymbol{\theta}, \boldsymbol{\phi}) = \ell_{\boldsymbol{\theta},\boldsymbol{\phi}}(\boldsymbol{x}_{\leq T}, \hat{\boldsymbol{h}}_{\leq T}) \cdot \nabla_{\boldsymbol{\phi}} \log q_{\boldsymbol{\phi}}(\hat{\boldsymbol{h}}_{\leq T}|\boldsymbol{x}_{\leq T}). \tag{16b}$$

This yields a doubly stochastic SGD update rule, summarized in Algorithm 2, whereby sampling is carried out both over the examples in the training set and over the hidden spike signals. Note that the rule (17) in Algorithm 2 can be translated into an on-line version as discussed in the previous section by introducing eligibility traces for the gradients of the log-probabilities in (16a)-(16b), and for the learning signal [16].

Choice of the variational distribution. Algorithm 2 applies with any choice of variational distribution $q_{\boldsymbol{\phi}}(\boldsymbol{h}_{\leq T}|\boldsymbol{x}_{\leq T})$, as long as it is feasible to sample from it and compute the gradient in (16b) as is. However, the locality properties and complexity of learning rule are strongly dependent on the choice of the variational distribution. We now discuss a specific choice considered in [8], [9], [19], [20], [26] that yields a simplified rule. Accordingly, the true posterior $p_{\boldsymbol{\theta}}(\boldsymbol{h}_{\leq T}|\boldsymbol{x}_{\leq T})$ is approximated with a "feedforward" distribution that ignores the stochastic dependence of the hidden spike signals $\boldsymbol{h}_t$ at time t on the future values of the observed spike signals $\boldsymbol{x}_{\leq T}$. The corresponding variational distribution can be written as

$$q_{\boldsymbol{\theta}^{\text{H}}}(\boldsymbol{h}_{\leq T}|\boldsymbol{x}_{\leq T}) = \prod_{t=1}^{T} p_{\boldsymbol{\theta}^{\text{H}}}(\boldsymbol{h}_t|\boldsymbol{x}_{\leq t-1}, \boldsymbol{h}_{\leq t-1}) = \prod_{l=1}^{L} \prod_{t=1}^{T} \prod_{i \in \mathcal{H}^{(l)}} p(h_{i,t}^{(l)}|u_{i,t}^{(l)}), \tag{18}$$

where $p(h_{i,t}^{(l)} = 1|u_{i,t}^{(l)}) = \sigma(u_{i,t}^{(l)})$ by (7) with $s_{i,t}^{(l)} = h_{i,t}^{(l)}$. We note that (18) is an approximation of the true posterior $p_{\boldsymbol{\theta}}(\boldsymbol{h}_{\leq T}|\boldsymbol{x}_{\leq T}) = \prod_{t=1}^{T} p_{\boldsymbol{\theta}}(\boldsymbol{h}_t|\boldsymbol{x}_{\leq T}, \boldsymbol{h}_{\leq t-1})$ since it neglects the correlation between variables

$\boldsymbol{h}_t$ and the future observed samples $\boldsymbol{x}_{\geq t}$. In (18), we have emphasized that the variational parameters $\boldsymbol{\phi}$ are tied to a subset of the model parameters as per the equality $\boldsymbol{\phi} = \boldsymbol{\theta}^{\text{H}}$. As a result, this choice of variational distribution does not include extra learnable parameters apart from the model parameters $\boldsymbol{\theta}$.

Learning rule. With the choice (18) for the variational posterior, Algorithm 2 yields a learning rule that follows the general three-factor update (9) with a specific learning signal. To elaborate, we consider here the case of no lateral connections, i.e., $\boldsymbol{r}^{(l)} = \mathbf{0}$ for all l. The more general case follows in a manner similar to the discussion in the previous section.

Each iteration of Algorithm 2 is realized by means of a feedforward sampling phase followed by the global feedback of a learning signal. First, in the *feedforward sampling phase*, each hidden neuron $i \in \mathcal{H}^{(l)}$ emits a spike, i.e., $\hat{h}_{i,t}^{(l)} = 1$, at any time t by following distribution (18), i.e., with probability $\sigma(\hat{u}_{i,t}^{(l)})$. The membrane potential $\hat{u}_{i,t}^{(l)}$ of any neuron i in the lth layer at time t is obtained from (1) with observed neurons clamped to the training example $\boldsymbol{x}_{\leq t-1}$ and hidden neurons clamped to the samples $\hat{\boldsymbol{h}}_{\leq t-1}$. Second, in the *global feedback phase*, a central processor collects the log-probabilities $p(x_{i,t}^{(l)}|\hat{u}_{i,t}^{(l)})$ from all observed neurons $i \in \mathcal{X}^{(l)}$, and feeds back the learning signal (14), which reads

$$\hat{\ell}_{\boldsymbol{\theta}^{\text{X}}}(\boldsymbol{x}_{\leq T}, \hat{\boldsymbol{h}}_{\leq T}) = \sum_{t=1}^{T} \log p_{\boldsymbol{\theta}^{\text{X}}}(\boldsymbol{x}_t|\boldsymbol{x}_{\leq t-1}, \hat{\boldsymbol{h}}_{\leq t-1}) = \sum_{l=1}^{L} \sum_{t=1}^{T} \sum_{i \in \mathcal{X}^{(l)}} \log p(x_{i,t}^{(l)}|\hat{u}_{i,t}^{(l)}), \tag{19}$$

to all latent neurons. Finally, the Monte Carlo approximated gradients (16) are computed locally at each neuron using the fully specified spike signals $\boldsymbol{s}_{\leq T} = (\boldsymbol{x}_{\leq T}, \hat{\boldsymbol{h}}_{\leq T})$. Specifically, each observed neuron $i \in \mathcal{X}^{(l)}$ computes the gradient $\nabla_{\boldsymbol{\theta}_i^{(l)}} \hat{L}_{\boldsymbol{x}_{\leq T}}(\boldsymbol{\theta})$ in (16a) with respect to its local parameters $\boldsymbol{\theta}_i^{(l)}$, while each hidden neuron $i \in \mathcal{H}^{(l)}$ computes the gradient $\nabla_{\boldsymbol{\theta}_i^{(l)}} \hat{L}_{\boldsymbol{x}_{\leq T}}(\boldsymbol{\theta})$ in (16b) using the global learning signal $\hat{\ell}_{\boldsymbol{\theta}^{\text{X}}}(\boldsymbol{x}_{\leq T}, \hat{\boldsymbol{h}}_{\leq T})$ in (19).

Interpretation. The gradient $\nabla_{w_{j,i}^{(l)}} \hat{L}_{\boldsymbol{x}_{\leq T}}(\boldsymbol{\theta})$ for a synaptic weight $w_{j,i}^{(l)}$ of any observed neuron $i \in \mathcal{X}^{(l)}$, obtained from (16a) and (8b), follows the two-factor rule described in the previous section. In contrast, the gradient $\nabla_{w_{j,i}^{(l)}} \hat{L}_{\boldsymbol{x}_{\leq T}}(\boldsymbol{\theta})$ of any hidden neuron $i \in \mathcal{H}^{(l)}$, computed from (16b) and (8b), applies a three-factor learning rule (9). Accordingly, the post-synaptic error signal of hidden neuron i and the filtered feedforward trace of pre-synaptic neuron j are multiplied by the global learning signal (19). The global learning signal can be interpreted as an internal reward signal. To see this, we can rewrite (19) as

$$\hat{\ell}_{\boldsymbol{\theta}^{\text{X}}}(\boldsymbol{x}_{\leq T}, \hat{\boldsymbol{h}}_{\leq T}) = \log p_{\boldsymbol{\theta}}(\boldsymbol{x}_{\leq T}|\hat{\boldsymbol{h}}_{\leq T}) - \log \frac{q_{\boldsymbol{\theta}^{\text{H}}}(\hat{\boldsymbol{h}}_{\leq T}|\boldsymbol{x}_{\leq T})}{p_{\boldsymbol{\theta}}(\hat{\boldsymbol{h}}_{\leq T})}. \tag{20}$$

According to (20), the learning signal rewards hidden spike signals $\hat{\boldsymbol{h}}_{\leq T}$ producing observations $\boldsymbol{x}_{\leq T}$ that yield a large likelihood $\log p_{\boldsymbol{\theta}}(\boldsymbol{x}_{\leq T}|\hat{\boldsymbol{h}}_{\leq T})$. Furthermore, it penalizes values of hidden spike signals $\hat{\boldsymbol{h}}_{\leq T}$ that have large variational probability $q_{\boldsymbol{\theta}^{\text{H}}}(\hat{\boldsymbol{h}}_{\leq T}|\boldsymbol{x}_{\leq T})$ while having a low prior probability $p_{\boldsymbol{\theta}}(\hat{\boldsymbol{h}}_{\leq T})$

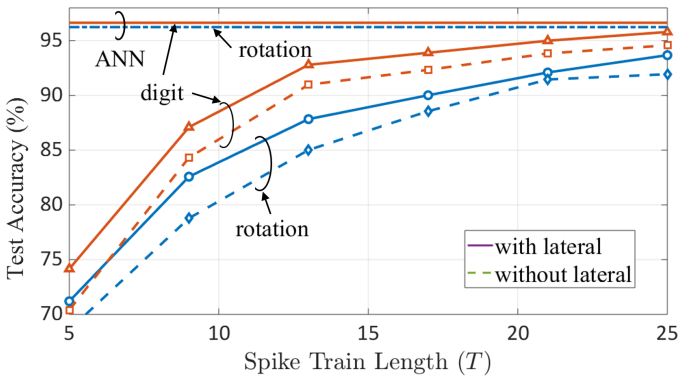

Fig. 4. Multi-task supervised learning based on an SNN with $L = 1$ trained via ML learning in Algorithm 1: classification accuracy for the two tasks of digit and orientation classification versus the duration T of the operation of the SNN. The performance of an ANN with the same topology is shown as a baseline.

under the model. This term acts as a regularizer, which ensures that the variational distribution is not too different from the prior [23, Ch. 6].

APPLICATIONS

In this section, we discuss some exemplifying applications of SNNs to supervised, unsupervised, and reinforcement learning.

Supervised Learning

Supervised learning aims at generalizing input-output patterns based on the observation of a training set $\{(a_m, o_m)\}_{m=1}^{M}$ of examples, where a_m is an input signal and o_m is the desired output. As discussed in the box "Spike-Domain Coding and Decoding", if the input a is a natural signal, such as an image, it should first be encoded in the spike domain, producing the input spike signals $\boldsymbol{s}_{\leq T}^{(0)}$ for the 0th layer (see the section "Models"). In a similar manner, focusing on classification, each output o should be associated with a subset of spatial-temporal configurations of the output spike signals. The simplest SNN to be used for classification has hence a two-layer architecture ($L = 1$), consisting of input (0th) and output (1th) layers. In this case, the behaviors of all neurons are fully observed and training can be done using Algorithm 1. If instead there are intermediate layers, i.e., $L > 1$, these layers are hidden and the learning rule in Algorithm 2 applies.

As an example, consider a multi-task learning problem, whereby, given a possibly rotated image of a handwritten digit, the SNN should both classify the handwritten number and detect whether a rotation is present or not. Assuming rate coding and rate decoding, Fig. 4, adapted from [24], shows the classification

accuracy for both tasks in the test set versus the duration T of the operation of the SNN, when a two-layer SNN with $K_\alpha = K_\beta = 2$ weights per synapse and neuron is trained using Algorithm 1. The classification accuracy of a conventional ANN with the same topology and a soft-max output layer is added for comparison. Note that, unlike the SNN, the ANN outputs real values, namely the logits for each class processed by the soft-max layer. It is seen that the SNN efficiently learns how to make use of the lateral correlations among output neurons participating in the same task in order to inhibit spikes from more than one neuron assigned to either a digit or a rotation value. Moreover, the SNN is seen to provide a graceful trade-off between accuracy and complexity. As T increases, the number of spikes that are processed and output by the SNN grows larger, entailing a larger inference complexity, but also an improved accuracy that tends to that of the reference ANN.

Unsupervised Learning

Unsupervised learning tasks include a variety of different problems ranging from density estimation to clustering and sample generation (see [23, Ch. 6]). Considering the latter as a typical application, a training set $\{a_m\}_{m=1}^M$ of examples is given, and the problem is that of training a machine that, ideally, outputs samples by mimicking the probabilistic mechanism underlying the generation of the training examples. For instance, if the training inputs are images of a certain type of subject, such as celebrities, the machine should output images similar to those in the training set. Upon conversion in the spike domain, each example a in the training set yields a spike signal $\boldsymbol{x}_{\leq T}$. Within the framework presented in the previous sections, an SNN generative model can be defined by considering an SNN whose last-layer spiking neurons are clamped to the spike signals in the training set, i.e., $\boldsymbol{s}_{\leq T}^{(L)} = \boldsymbol{x}_{\leq T}$. All the previous layers are instead considered as hidden variables that aid the generation of the samples at the last layer. Neurons in layer 0 are fixed to some arbitrary sequence, e.g., all-zero. Training can be carried out by following Algorithm 2.

As an example, consider the generation of binary handwritten digit images using an SNN with $L = 2$. The variational distribution $q_{\boldsymbol{\phi}}(\boldsymbol{h}_{\leq T}|\boldsymbol{x}_{\leq T})$ defines the probability of the spike signals $\boldsymbol{h}_{\leq T}$ output by the neurons in layer 1 given the spike-domain encoded image $\boldsymbol{x}_{\leq T}$ assigned to layer $L = 2$. We select this probability here to be a GLM as the forward model $p_{\boldsymbol{\theta}}(\boldsymbol{x}_{\leq T}|\boldsymbol{h}_{\leq T})$ but with different synaptic weights and biases in the variational parameter vector $\boldsymbol{\phi}$. No lateral connections are assumed. The variational model, once trained, can be used to define a probabilistic map between the spike-domain input image and a hidden spike-domain representation $\boldsymbol{h}_{\leq T}$. Here we take the number of hidden neurons to be half of the number of input neurons. Fig. 5 shows the resulting reconstruction error, measured in terms of the percentage of pixels recovered incorrectly, that is obtained by passing the representation $\boldsymbol{h}_{\leq T}$ through

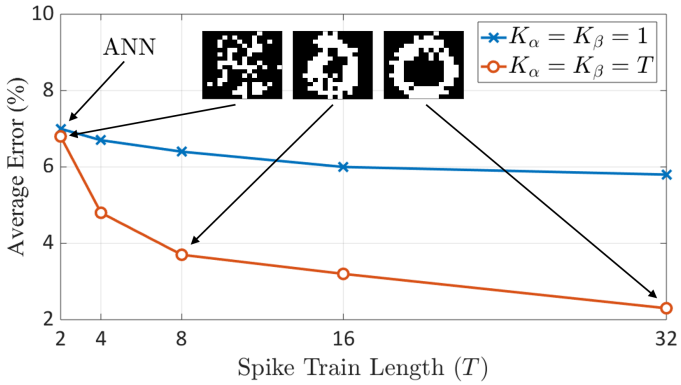

Fig. 5. Unsupervised learning based on an SNN with $L = 2$ trained via variational learning in Algorithm 2: reconstruction error, measured in terms of the percentage of pixels recovered incorrectly, and sample images generated by the trained SNN versus the duration T of the operation of the SNN. The performance of an ANN with the same topology and soft-max functions is shown as a baseline.

the forward SNN model. The image is decoded using rate decoding by thresholding the firing rates. For reference, we also plot the error of an ANN with the same topology and soft-max functions for both direct and variational distributions. The figure shows that, as a generator of binary images, SNNs can be more effective than the counterpart ANN, with a gain that increases as the operation T and the number of synaptic weights K_α and K_β increases. This gain is due to the increased robustness to noise obtained as T grows larger, as well as to the larger model capacity with increased K_α and K_β, which enables learning of the synaptic and feedback filters. This will be further discussed below.

Reinforcement Learning

In reinforcement learning, data is generated by an agent as it interacts with an environment [27]. At every step $\tau = 1, 2, \dots$ of the learning process, the agent observes the current state variable s_τ and takes an action a_τ from a finite set. As a result, it receives feedback from the environment in the form of a reward signal r_τ that measures the immediate return accrued from the action taken. The action also generally affects the next state of the system $s_{\tau+1}$, and the process repeats until some condition is satisfied, ending a learning episode. The goal of learning across multiple episodes is that of maximizing the average discounted return $G = \sum_{\tau=0}^{\infty} \gamma^\tau r_\tau$ with some discounting factor $\gamma \leq 1$. A prototypical example is that of an agent exploring a grid-world with the aim of reaching a goal point, hence ending an episode, while dealing with unknown "wind" conditions in different positions of the grid [27].

Probabilistic SNNs can be directly used to define a stochastic policy mapping input state s_τ to action a_τ with its learnable parameters. An SNN can be used for this purpose by encoding the state s_τ into the 0th layer spike signals $\boldsymbol{s}_{\leq T}^{(0)}$ and action a_τ into the Lth layer outputs $\boldsymbol{s}_{\leq T}^{(L)}$ in a manner akin to supervised

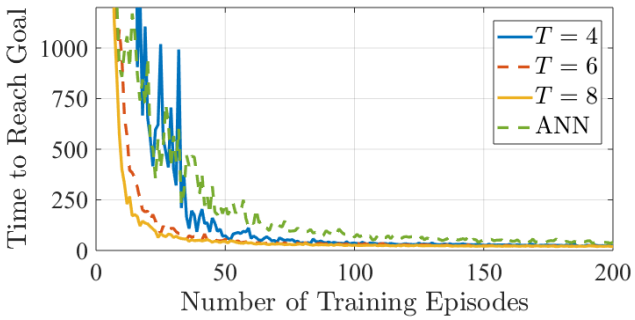

Fig. 6. Application of reinforcement learning based on a first-to-spike SNN with $L = 1$ as a stochastic random policy: time needed to reach the goal state as a function of the number of training episodes.

learning [28], [29]. Unlike supervised learning, however, here the output action a_τ is not pre-specified by the training data, but is rather the result of past decisions of the agent. Nevertheless, for given actions a_τ, if an SNN with $L = 1$ is used, the behavior of the SNN can be considered to be fully observed, while hidden layers exist when $L > 1$. Training can be carried out in a manner similar to Algorithms 1 and 2, respectively, by leveraging the policy gradient strategy [27, Ch. 13]. Accordingly, the parameter updates in (10) and (17b) are multiplied by a global reward signal accounting for the returns obtained in a given episode [29, Algorithm 1]. This renders the update (10) of the synaptic weights a three-factor rule following (9).

An example is shown in Fig. 6 from [29], which considers the grid-world example mentioned above and plots the time needed to reach the goal point as a function of the number of training episodes for a two-layer SNN with $K_\alpha = K_\beta = 4$ basis functions, as well as for an ANN with the same topology. It can be observed that in this example, the ANN policy is outperformed by the SNN policy. This is due to the capability of SNNs to optimize temporal processing by learning the synaptic and feedback filters. This increases the capacity of the model, hence, potentially improving the performance.

Conclusions and Open Problems

This paper has presented a review of models and training methods for probabilistic SNNs within a statistical signal processing framework. The SNN architectures considered in this paper are of feedforward nature, but probabilistic SNN models can naturally accommodate more general topologies with recurrent connections among neurons, allowing the implementation of long-term memory mechanisms [30]. Furthermore, an alternative to the models studied here prescribes the retrieval of information from the emergent steady-state behavior of the SNN – an approach also known as neural sampling [2], [22], [30]. Interesting open problems include *meta-learning*, whereby the goal is to learning how to train or

adapt a network to a new task (see, e.g., [30]), and the definition of efficient input/ output (I/O) interfaces for SNNs.

REFERENCES

[1] H. Paugam-Moisy and S. Bohte, "Computing with spiking neuron networks," in *Handbook of Natural Computing*. Springer, 2012, pp. 335–376.

[2] M. Davies et al., "Loihi: A neuromorphic manycore processor with on-chip learning," *IEEE Micro*, 2018.

[3] J. H. Lee, T. Delbruck, and M. Pfeiffer, "Training deep spiking neural networks using backpropagation," *Frontiers in Neuroscience*, vol. 10, p. 508, 2016.

[4] P. O'Connor and M. Welling, "Deep spiking networks," *arXiv preprint arXiv:1602.08323*, 2016.

[5] Y. Wu, L. Deng, G. Li, J. Zhu, and L. Shi, "Spatio-temporal backpropagation for training high-performance spiking neural networks," *Frontiers in Neuroscience*, vol. 12, 2018.

[6] W. Gerstner and W. M. Kistler, *Spiking neuron models: Single neurons, populations, plasticity*. Cambridge university press, 2002.

[7] J. W. Pillow, J. Shlens, L. Paninski, A. Sher, A. M. Litke, E. Chichilnisky, and E. P. Simoncelli, "Spatio-temporal correlations and visual signalling in a complete neuronal population," *Nature*, vol. 454, no. 7207, p. 995, 2008.

[8] T. Osogami, "Boltzmann machines for time-series," *arXiv preprint arXiv:1708.06004*, 2017.

[9] D. Kappel, S. Habenschuss, R. Legenstein, and W. Maass, "Network plasticity as Bayesian inference," *PLoS Computational Biology*, vol. 11, no. 11, p. e1004485, 2015.

[10] B. Gardner, I. Sporea, and A. Grüning, "Learning spatiotemporally encoded pattern transformations in structured spiking neural networks," *Neural Computation*, vol. 27, no. 12, pp. 2548–2586, 2015.

[11] D. Dold et al., "Stochasticity from function-why the bayesian brain may need no noise," *arXiv preprint arXiv:1809.08045*, 2018.

[12] S. Thorpe, A. Delorme, and R. Van Rullen, "Spike-based strategies for rapid processing," *Neural Networks*, vol. 14, no. 6-7, pp. 715–725, 2001.

[13] A. A. Lazar and L. T. Tóth, "Perfect recovery and sensitivity analysis of time encoded bandlimited signals," *IEEE Transactions on Circuits and Systems I: Regular Papers*, vol. 51, no. 10, pp. 2060–2073, 2004.

[14] A. A. Faisal, L. P. Selen, and D. M. Wolpert, "Noise in the nervous system," *Nature Reviews Neuroscience*, vol. 9, no. 4, p. 292, 2008.

[15] N. Frémaux and W. Gerstner, "Neuromodulated spike-timing-dependent plasticity, and theory of three-factor learning rules," *Frontiers in Neural Circuits*, vol. 9, p. 85, 2016.

[16] J. Brea, W. Senn, and J.-P. Pfister, "Matching recall and storage in sequence learning with spiking neural networks," *Journal of Neuroscience*, vol. 33, no. 23, pp. 9565–9575, 2013.

[17] I. Goodfellow, Y. Bengio, A. Courville, and Y. Bengio, *Deep learning*. MIT press Cambridge, 2016, vol. 1.

[18] E. L. Bienenstock, L. N. Cooper, and P. W. Munro, "Theory for the development of neuron selectivity: orientation specificity and binocular interaction in visual cortex," *Journal of Neuroscience*, vol. 2, no. 1, pp. 32–48, 1982.

[19] J. Brea, W. Senn, and J.-P. Pfister, "Sequence learning with hidden units in spiking neural networks," in *Advances in Neural Information Processing Systems*, 2011, pp. 1422–1430.

[20] D. J. Rezende and W. Gerstner, "Stochastic variational learning in recurrent spiking networks," *Frontiers in Computational Neuroscience*, vol. 8, p. 38, 2014.

[21] A. J. Watt and N. S. Desai, "Homeostatic plasticity and STDP: keeping a neuron's cool in a fluctuating world," *Frontiers in Synaptic Neuroscience*, vol. 2, p. 5, 2010.

[22] L. Buesing, J. Bill, B. Nessler, and W. Maass, "Neural dynamics as sampling: a model for stochastic computation in recurrent networks of spiking neurons," *PLoS Computational Biology*, vol. 7, no. 11, p. e1002211, 2011.

[23] O. Simeone, "A brief introduction to machine learning for engineers," *Foundations and Trends® in Signal Processing*, vol. 12, no. 3-4, pp. 200–431, 2018.

[24] H. Jang and O. Simeone, "Training dynamic exponential family models with causal and lateral dependencies for generalized neuromorphic computing," *arXiv preprint arXiv:1810.08940*, 2018.

[25] A. Mnih and K. Gregor, "Neural variational inference and learning in belief networks," in *International Conference on Machine Learning*, 2014, pp. 1791–1799.

[26] G. E. Hinton and A. D. Brown, "Spiking boltzmann machines," in *Advances in Neural Information Processing Systems*, 2000, pp. 122–128.

[27] R. S. Sutton and A. G. Barto, *Reinforcement learning: An introduction*. MIT press, 2018.

[28] N. Frémaux, H. Sprekeler, and W. Gerstner, "Reinforcement learning using a continuous time actor-critic framework with spiking neurons," *PLoS Computational Biology*, vol. 9, no. 4, p. e1003024, 2013.

[29] B. Rosenfeld, O. Simeone, and B. Rajendran, "Learning first-to-spike policies for neuromorphic control using policy gradients," *arXiv preprint arXiv:1810.09977*, 2018.

[30] G. Bellec, D. Salaj, A. Subramoney, R. Legenstein, and W. Maass, "Long short-term memory and learning-to-learn in networks of spiking neurons," *arXiv preprint arXiv:1803.09574*, 2018.